



## Research paper

# Treatment of cadmium(II) and zinc(II) with N<sub>2</sub>-donor linkages in presence of β-diketone ligand; supported by structural, spectral, theoretical and docking studies

Farzin Marandi<sup>a,\*</sup>, Keyvan Moeini<sup>a,\*</sup>, Fereshteh Alizadeh<sup>a</sup>, Zahra Mardani<sup>b</sup>, Ching Kheng Quah<sup>c</sup>, Wan-Sin Loh<sup>c</sup>, J. Derek Woollins<sup>d</sup>

<sup>a</sup> Chemistry Department, Payame Noor University, 19395-4697 Tehran, Islamic Republic of Iran

<sup>b</sup> Inorganic Chemistry Department, Faculty of Chemistry, Urmia University, 57561-51818 Urmia, Islamic Republic of Iran

<sup>c</sup> X-ray Crystallography Unit, School of Physics, Universiti Sains Malaysia, 11800 USM, Penang, Malaysia

<sup>d</sup> EaStCHEM School of Chemistry, University of St Andrews, St Andrews Fife UK, KY16 9ST, United Kingdom

## ARTICLE INFO

## Keywords:

Cadmium(II)  
Nitrogen donor linker  
DFT study  
Docking study  
Coordination polymer

## ABSTRACT

Five compounds,  $\{(\mu\text{-OAc})(\text{DPPD})\text{Cd}(\mu\text{-PYZ})\text{Cd}(\text{DPPD})(\mu\text{-OAc})\}_n$  (**1**); HDPPD: 1,3-diphenylpropane-1,3-dione; PYZ: pyrazine,  $\{\text{Cd}(\mu\text{-4,4'-Bipy})(\text{DPPD})_2\}_n$  (**2**); Bipy: bipyridine  $[(\text{DPPD})_2\text{Zn}(\mu\text{-4,4'-Bipy})\text{Zn}(\text{DPPD})_2]$  (**3**),  $\{\text{Cd}(\mu\text{-DPP})(\text{DPPD})_2\}_n$  (**4**); DPP: 1,3-di(pyridin-4-yl)propane and (*Z*)-3-hydroxy-1,3-bis(4-methoxyphenyl)prop-2-en-1-one (*Z*-HMPP), were prepared and identified by elemental analysis, FT-IR, <sup>1</sup>H NMR spectroscopy and single-crystal X-ray diffraction. **1,2** and **4** form 1D coordination polymers whereas **3** adopts a binuclear structure with the zinc atom in a distorted square-pyramidal geometry. In addition to these complexes, the enolic structure of the *Z*-HMPP is reported. The ability of compounds to interact with the nine biomacromolecules (BRAF kinase, CatB, DNA gyrase, HDAC7, rHA, RNR, TrxR, TS and Top II) is investigated by the Docking calculations (for **3** and its ligands). The charge distribution pattern of the optimized structure of **3** was studied by NBO analysis. The Polymer Stability Slope for pentameric chain (PSS<sup>5</sup>, new parameter which is proposed in this paper) of the coordination polymers of **1, 2** and **4** were calculated to investigate the variation of energy level during the growing the polymer chain in the solid phase.

## 1. Introduction

Coordination polymers are interesting metal-organic hybrid materials in which metal ions or metal-containing clusters act as nodes and organic ligands act as spacers; both units are linked via coordination bonds to form one-, two- or three-dimensional extended structures [1]. This class of compounds has been used as electrodes in supercapacitors [2], gas storage/separation and ion exchange [3–8], biological and material science [9,10], sensing [11–15], precursors for the preparation of nano-materials [16], magnetism [17–21], luminescent materials nonlinear optics [22–25], catalysis [26–29],

Aromatic β-diketones are frequently used as chelating ligands for Lewis acids and to produce complexes used in many applications such as catalysis [30], vapour deposition [31], luminescent compounds [32,33], near infrared organic light emitting devices [34,35] and optoelectronics [36]. For example, difluoroboron diketonates [37] have lately received tremendous attention due to their mechanochromic

luminescence (ML) [38] and room-temperature phosphorescence properties [39–41]. Some 1D-, 2D- and 3D-coordination polymers containing β-diketone derivatives have been reported [42,43].

In order to extend the chemistry of these coordination polymers, in this work, the synthesis of compounds including,  $\{(\mu\text{-OAc})(\text{DPPD})\text{Cd}(\mu\text{-PYZ})\text{Cd}(\text{DPPD})(\mu\text{-OAc})\}_n$  (**1**); HDPPD: 1,3-diphenylpropane-1,3-dione (Scheme 1); PYZ: pyrazine (Scheme 1),  $\{\text{Cd}(\mu\text{-4,4'-Bipy})(\text{DPPD})_2\}_n$  (**2**); Bipy: bipyridine (Scheme 1),  $[(\text{DPPD})_2\text{Zn}(\mu\text{-4,4'-Bipy})\text{Zn}(\text{DPPD})_2]$  (**3**),  $\{\text{Cd}(\mu\text{-DPP})(\text{DPPD})_2\}_n$  (**4**); DPP: 1,3-di(pyridin-4-yl)propane (Scheme 1) and (*Z*)-3-hydroxy-1,3-bis(4-methoxyphenyl)prop-2-en-1-one (*Z*-HMPP), are described, along with the characterization and theoretical study of the compounds.

In addition to the expected biological properties of compounds containing β-diketones [44,45] and pyridine derivatives [46–49], binding of the zinc(II) ion to this unit make these complexes as a good choice for biologically active compounds [50–52], thus docking calculations were run to investigate the possibility of interaction between

\* Corresponding authors.

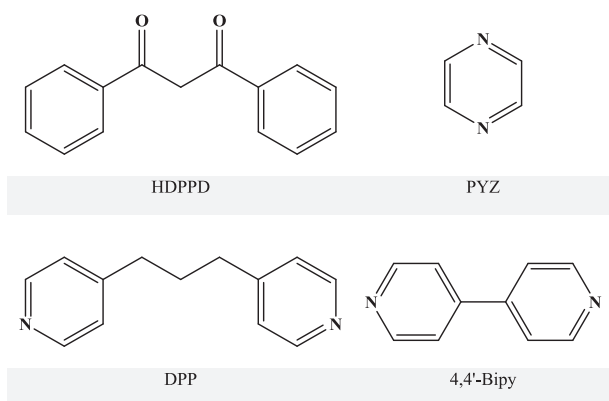
E-mail addresses: [f.marandi@gmail.com](mailto:f.marandi@gmail.com) (F. Marandi), [k1\\_moeini@yahoo.com](mailto:k1_moeini@yahoo.com) (K. Moeini).

<https://doi.org/10.1016/j.ica.2018.07.014>

Received 25 April 2018; Received in revised form 6 July 2018; Accepted 6 July 2018

Available online 11 July 2018

0020-1693/ © 2018 Elsevier B.V. All rights reserved.



**Scheme 1.** Structures of the 1,3-diphenylpropane-1,3-dione (HDPPD), pyrazine (PYZ), 4,4'-bipyridine (4,4'-Bipy) and 1,3-di(pyridin-4-yl)propane (DPP) ligands.

**3** and its ligands (4,4'-bipyridine and DPPD) with the nine protein targets, including: BRAF kinase, Cathepsin B (CatB), DNA gyrase, Histone deacetylase (HDAC7), recombinant Human albumin (rHA), Ribonucleotide reductases (RNR), Thioredoxin reductase (TrxR), Thymidylate synthase (TS), Topoisomerase II (Top II). These proteins are used in this project either due to their reported roles in the cancer growth or as transport agents that affect drug pharmacokinetic properties (e.g., rHA). Also, DNA gyrase was included to study the possibility of the compounds also acting as antimalarial agents [53].

## 2. Experimental

### 2.1. Materials and instrumentation

All starting chemicals and solvents were reagent or analytical grade and used as received. Infrared spectra in the range 4000–400  $\text{cm}^{-1}$  were recorded on KBr pellets with a FT-IR 8400-Shimadzu spectrometer.  $^1\text{H}$  NMR spectra were recorded on a Bruker spectrometer at 250 MHz; chemical shifts  $\delta$  are given in parts per million, relative to TMS as an internal standard. The carbon, hydrogen and nitrogen contents were determined in a Thermo Finnigan Flash Elemental Analyzer 1112 EA. Melting points were determined with a Barnsted Electrothermal 9200 electrically heated apparatus.

#### 2.1.1. Synthesis of $\{(\mu\text{-OAc})(\text{DPPD})\text{Cd}(\mu\text{-PYZ})\text{Cd}(\text{DPPD})(\mu\text{-OAc})\}_n$ (**1**)

HDPPD (0.135 g, 0.6 mmol), pyrazine (0.072 g, 0.9 mmol) and Cd(OAc) $_2$ ·2H $_2$ O (0.080 g, 0.3 mmol) were placed in the large arms of a branched tube (see ref [54]). Ethanol was carefully added to fill both arms. The tube was then sealed and the ligand-containing arm was immersed in a bath at 60 °C while the other arm was maintained at ambient temperature [55]. After a few days, the colorless crystals deposited in the cooler arm were filtered off and dried in air. Yield: 0.058 g, 45%; m. p. 212–217 °C. Anal. Calcd for C $_{19}$ H $_{16}$ CdNO $_4$  (434.73): C, 52.49; H, 3.71; N, 3.22. Found: C, 52.62; H, 3.75; N, 3.19%. IR (KBr,  $\text{cm}^{-1}$ ): 3105 w ( $\nu$  CH) $^{\text{ar}}$ , 3063 w ( $\nu$  CH) $^{\beta\text{-diketone}}$ , 2997 w ( $\nu$  CH), 1592 s ( $\nu$  C=C +  $\nu$  C=O) $^{\beta\text{-diketone}}$ , 1580 m ( $\nu$  C=N), 1543 m ( $\nu_{\text{as}}$  COO) $^{\text{OAc}}$ , 1522 m ( $\nu$  C=O +  $\nu$  C=C), 1456 w ( $\nu$  C=C) $^{\text{ar}}$  and/or  $\delta_{\text{as}}$  CH $_3$ ), 1434 m ( $\nu_{\text{s}}$  COO) $^{\text{OAc}}$  and/or  $\delta$  CH +  $\nu$  C=C $^{\beta\text{-diketone}}$ , 1343 w ( $\delta_{\text{s}}$  CH $_2$ ), 674 ( $\delta$  OCO) $^{\text{OAc}}$ .  $^1\text{H}$  NMR (250 MHz, DMSO- $d_6$ , ppm, Hz):  $\delta$  = 8.64)s, 2 H, pyrazine, 7.40–7.91)m, 10 H, phenyl-DPPD, 6.54)s, 1 H,  $\beta$ -diketone, 1.82)s, 3H, OAc).

#### 2.1.2. Synthesis of $\{\text{Cd}(\mu\text{-4,4'-Bipy})(\text{DPPD})_2\}_n$ (**2**)

The procedure for synthesis of **2** was similar to **1** except that pyrazine was replaced by 4,4'-bipyridine (0.141 g, 0.9 mmol) using the MeOH/H $_2$ O in a ratio of 3:1. Yield: 0.028 g, 13%; m. p. 204–214 °C. Anal. Calcd for C $_{40}$ H $_{30}$ CdN $_2$ O $_4$  (715.06): C, 67.18; H, 4.23; N, 3.92.

Found: C, 67.32; H, 4.28; N, 4.01%. IR (KBr,  $\text{cm}^{-1}$ ): 3091 w ( $\nu$  CH) $^{\text{ar}}$ , 3056 w ( $\nu$  CH) $^{\beta\text{-diketone}}$ , 1597 s ( $\nu$  C=C +  $\nu$  C=O) $^{\beta\text{-diketone}}$ , 1552 m ( $\nu$  C=O +  $\nu$  C=C) $^{\beta\text{-diketone}}$ , 1513 m ( $\nu$  C=N), 1477 m ( $\nu$  C=C) $^{\text{ar}}$ , 1454 s ( $\delta$  CH +  $\nu$  C=C) $^{\beta\text{-diketone}}$ .  $^1\text{H}$  NMR (250 MHz, DMSO- $d_6$ , ppm, Hz):  $\delta$  = 8.69–8.71)d, 4 H, 4,4'-bipy, 7.90–8.17)m, 8 H, DPPD, 7.79–7.81)d, 4 H, 4,4'-bipy, 7.33–7.66)m, 12H, DPPD, 6.54)s, 2 H,  $\beta$ -diketone).

#### 2.1.3. Synthesis of $[(\text{DPPD})_2\text{Zn}(\mu\text{-4,4'-Bipy})\text{Zn}(\text{DPPD})_2]$ (**3**)

The procedure for synthesis of **3** was similar to **2** except that Cd(OAc) $_2$ ·2H $_2$ O was replaced by Zn(OAc) $_2$ ·2H $_2$ O (0.066 g, 0.3 mmol) using the MeOH/EtOH in a ratio of 3:1. Yellowish crystals were formed after a few days in the cooler arm and filtered. Yield: 0.026 g, 15%; m. p. 237–238 °C. Anal. Calcd for C $_{70}$ H $_{52}$ N $_2$ O $_8$ Zn $_2$  (1179.87): C, 71.25; H, 4.44; N, 2.37. Found: C, 71.51; H, 4.53; N, 2.35%. IR (KBr,  $\text{cm}^{-1}$ ): 3102 w ( $\nu$  CH) $^{\text{ar}}$ , 3066 w ( $\nu$  CH) $^{\beta\text{-diketone}}$ , 1606 m ( $\nu$  C=C +  $\nu$  C=O) $^{\beta\text{-diketone}}$ , 1555 m ( $\nu$  C=O +  $\nu$  C=C) $^{\beta\text{-diketone}}$ , 1544 m ( $\nu$  C=N), 1474 s ( $\nu$  C=C) $^{\text{ar}}$ , 1458 s ( $\delta$  CH +  $\nu$  C=C) $^{\beta\text{-diketone}}$ .  $^1\text{H}$  NMR (250 MHz, DMSO- $d_6$ , ppm, Hz):  $\delta$  = 8.73)d, 2H, 4,4'-bipy, 8.02–8.05)d, 8 H, DPPD, 7.80–7.82)d, 2 H, 4,4'-bipy, 7.46–7.48)m, 12 H, DPPD, 6.76)s, 2 H,  $\beta$ -diketone).

#### 2.1.4. Synthesis of $\{\text{Cd}(\mu\text{-DPP})(\text{DPPD})_2\}_n$ (**4**)

The procedure for synthesis of **4** was similar to **1** except that pyrazine was replaced by DPP (0.178 g, 0.9 mmol) using the MeOH/EtOH in a ratio of 1:3. After one week, the reaction mixture was filtered and then colorless crystals suitable for X-ray diffraction studies were obtained by slow evaporation after a few days. Yield: 0.017 g, 8%; m. p. 215 °C. Anal. Calcd for C $_{43}$ H $_{36}$ CdN $_2$ O $_4$  (757.14): C, 68.21; H, 4.79; N, 3.70. Found: C, 67.94; H, 4.77; N, 3.71%. IR (KBr,  $\text{cm}^{-1}$ ): 3087 w ( $\nu$  CH) $^{\text{ar}}$ , 3060 w ( $\nu$  CH) $^{\beta\text{-diketone}}$ , 2945 w ( $\nu$  CH $_2$ ), 1594 s ( $\nu$  C=C +  $\nu$  C=O) $^{\beta\text{-diketone}}$ , 1547 m ( $\nu$  C=O +  $\nu$  C=C) $^{\beta\text{-diketone}}$ , 1515 m ( $\nu$  C=N), 1478 m ( $\nu$  C=C) $^{\text{ar}}$ , 1455 s ( $\delta$  CH +  $\nu$  C=C) $^{\beta\text{-diketone}}$ , 1406 s ( $\delta_{\text{as}}$  CH $_2$ ), 1301 w ( $\delta_{\text{s}}$  CH $_2$ ).  $^1\text{H}$  NMR (250 MHz, DMSO- $d_6$ , ppm, Hz):  $\delta$  = 8.43–8.45)d, 4H, DPP, 7.89–7.91)d, 8H, DPPD, 7.41)m, 12 H, DPPD, 7.22–7.24)m, 4 H, DPP, 6.53)s, 2 H,  $\beta$ -diketone, 2.56–2.63 (t, 4 H, DPP), 1.87–1.93 (m, 2 H, DPP).

#### 2.1.5. Preparation of (Z)-3-hydroxy-1,3-bis(4-methoxyphenyl)prop-2-en-1-one (Z-HMPP)

The procedure for synthesis of Z-HMPP was similar to **3** except that HDPPD and pyrazine was replaced by 1,3-bis(4-methoxyphenyl)propane-1,3-dione, HMPP (0.171 g, 0.6 mmol), and 1,2-di(pyridin-4-yl)ethane, DPE (0.164 g, 0.9 mmol), using the MeOH. After a few days, yellow crystals that were deposited in the cooler arm were filtered off and dried in air. Yield: 0.050 g; m. p. 222 °C. Anal. Calcd for C $_{17}$ H $_{16}$ O $_4$  (284.30): C, 71.82; H, 5.67. Found: C, 71.96; H, 5.66%. IR (KBr,  $\text{cm}^{-1}$ ): 3060 w ( $\nu$  CH) $^{\text{ar}}$ , 2962 w ( $\nu$  CH $_3$ ), 1604 s ( $\nu$  C=O) $^{\text{enol}}$ , 1545 w ( $\nu$  C=C) $^{\text{enol}}$ , 1491 m and 1458 w ( $\nu$  C=C) $^{\text{ar}}$ , 1438 m ( $\delta_{\text{as}}$  CH $_3$ ), 1303 m ( $\nu$  C–O) $^{\text{enol}}$  and/or  $\delta_{\text{s}}$  CH $_3$ ).  $^1\text{H}$  NMR (250 MHz, DMSO- $d_6$ , ppm, Hz):  $\delta$  = 8.10–8.13)d, 4 H, Ph, 7.51)s, 1 H,  $\beta$ -diketone, 7.17)s, 1 H, OH, 7.05–7.08)d, 4 H, Ph, 3.82–3.84 (s, 6 H, methoxy).

## 2.2. Crystal structure determination

Suitable crystals of **1–4** and Z-HMPP were chosen and their X-ray analysis were done using Apex-II Duo CCD diffractometer with fine-focus sealed tube graphite-monochromated Mo- $K\alpha$  radiation ( $\lambda$  = 0.71073 Å) at room temperature. The data was processed with SAINT and corrected for absorption using SADABS [56]. The structures were solved by direct method using the program SHELXTL [57] and were refined by full-matrix least squares technique on  $F^2$  using anisotropic displacement parameters for all non-hydrogen atoms. Diagrams of the molecular structure and unit cell were created using Ortep-III [58,59] and Diamond [60] softwares. Details of crystal data, data collection, structure solutions and refinements are given in Table 1. Selected bond lengths and angles of complexes are listed in Table 2 and hydrogen bond geometries in Table S2 (Supplementary Materials).

**Table 1**  
Crystal data and structure refinement for complexes of 1–4 and Z-HMPP.

	Z-HMPP	Complex 1	Complex 2	Complex 3	Complex 4
Empirical formula	C <sub>17</sub> H <sub>16</sub> O <sub>4</sub>	C <sub>19</sub> H <sub>16</sub> CdNO <sub>4</sub>	C <sub>40</sub> H <sub>30</sub> CdN <sub>2</sub> O <sub>4</sub>	C <sub>70</sub> H <sub>52</sub> N <sub>2</sub> O <sub>8</sub> Zn <sub>2</sub>	C <sub>43</sub> H <sub>36</sub> CdN <sub>2</sub> O <sub>4</sub>
Formula weight, g mol <sup>-1</sup>	284.30	434.73	715.06	1179.87	757.14
Crystal size, mm <sup>3</sup>	0.78 × 0.26 × 0.14	0.35 × 0.18 × 0.03	0.69 × 0.37 × 0.08	0.66 × 0.12 × 0.05	0.40 × 0.35 × 0.16
Temperature, K	296	296	296	296	296
Crystal system	monoclinic	triclinic	Orthorhombic	monoclinic	monoclinic
Space group	P2 <sub>1</sub> /n	P $\bar{1}$	Aba2	P2 <sub>1</sub> /c	C2/c
Unit cell dimensions (Å, °)					
<i>a</i>	4.1858(6)	6.5640(19)	10.9938(9)	10.8018(14)	13.1149(11)
<i>b</i>	10.2691(16)	9.733(3)	25.63a5(3)	28.923(4)	30.534(3)
<i>c</i>	32.589(5)	15.095(4)	11.8497(10)	18.183(2)	10.8920(9)
$\alpha$		94.274(6)			
$\beta$	90.758(3)	102.239		93.739(2)	125.236(1)
$\gamma$		109.674(4)			
Volume, Å <sup>3</sup>	1400.7(4)	876.2(4)	3339.5(5)	5668.6(13)	3562.5(5)
<i>Z</i>	4	2	4	4	4
Calculated density, g cm <sup>-3</sup>	1.348	1.648	1.422	1.383	1.412
Absorption coefficient, mm <sup>-1</sup>	0.10	1.27	0.70	0.91	0.66
<i>F</i> (0 0 0), e	600	434	1456	2440	1552
2 $\theta$ range for data collection (°)	4.6–44.8	5.0–50.8	4.8–58.2	4.4–33.6	5.4–49.4
<i>h</i> , <i>k</i> , <i>l</i> ranges	–5 ≤ <i>h</i> ≤ 5, –13 ≤ <i>k</i> ≤ 13, –44 ≤ <i>l</i> ≤ 44	–8 ≤ <i>h</i> ≤ 7, –11 ≤ <i>k</i> ≤ 11, –18 ≤ <i>l</i> ≤ 18	–14 ≤ <i>h</i> ≤ 15, –35 ≤ <i>k</i> ≤ 35, –16 ≤ <i>l</i> ≤ 16	–13 ≤ <i>h</i> ≤ 13, –36 ≤ <i>k</i> ≤ 36, –23 ≤ <i>l</i> ≤ 23	–17 ≤ <i>h</i> ≤ 17, –41 ≤ <i>k</i> ≤ 41, –14 ≤ <i>l</i> ≤ 14
Reflections collected/independent/ <i>R</i> <sub>int</sub>	28,663/3717/0.036	3296/3296/	33,979/4496/0.034	117,745/12,379/0.142	42,213/4791/0.031
Data/ref. parameters	3717/196	3296/229	4496/215	12,379/739	4791/252
Goodness-of-fit on <i>F</i> <sup>2</sup>	1.04	1.11	1.05	1.00	1.03
Final <i>R</i> indexes [ <i>I</i> > 2 $\sigma$ ( <i>I</i> )]	<i>R</i> <sub>1</sub> = 0.047, <i>wR</i> <sub>2</sub> = 0.127	<i>R</i> <sub>1</sub> = 0.040, <i>wR</i> <sub>2</sub> = 0.092	<i>R</i> <sub>1</sub> = 0.027, <i>wR</i> <sub>2</sub> = 0.063	<i>R</i> <sub>1</sub> = 0.054, <i>wR</i> <sub>2</sub> = 0.094	<i>R</i> <sub>1</sub> = 0.050, <i>wR</i> <sub>2</sub> = 0.141
Final <i>R</i> indexes [all data]	<i>R</i> <sub>1</sub> = 0.087, <i>wR</i> <sub>2</sub> = 0.150	<i>R</i> <sub>1</sub> = 0.045, <i>wR</i> <sub>2</sub> = 0.095	<i>R</i> <sub>1</sub> = 0.037, <i>wR</i> <sub>2</sub> = 0.069	<i>R</i> <sub>1</sub> = 0.148, <i>wR</i> <sub>2</sub> = 0.131	<i>R</i> <sub>1</sub> = 0.063, <i>wR</i> <sub>2</sub> = 0.154
Largest diff. peak/hole, e Å <sup>-3</sup>	0.12/–0.14	1.21/–0.56	0.41/–0.26	0.29/–0.23	0.62/–0.66

### 2.3. Computational details

All structures were optimized with the Gaussian 09 software [61] and calculated for an isolated molecule using Density Functional Theory (DFT) [62] at the B3LYP/LanL2DZ level of theory for complex 3 as well as for NBO analysis and B3LYP/6-31+G for Z-HMPP and HDPPD isomers. Cif files of complex 3 and Z-HMPP were used as input file for theoretical calculations.

### 2.4. Docking details

The pdb files 4r5y, 3ai8, 5cdn, 3c0z, 2bx8, 1peo, 3qfa, 1njb, 4gfh for the nine receptors, BRAF kinase, Cathepsin B (CatB), DNA gyrase,

Histone deacetylase (HDAC7), recombinant Human albumin (rHA), Ribonucleotide reductases (RNR), Thioredoxin reductase (TrxR), Thymidylate synthase (TS), Topoisomerase II (Top II), respectively, used in this research were obtained from the Protein Data Bank (pdb) [59]. The obtained full version of Genetic Optimisation for Ligand Docking (GOLD) 5.5 [63] was used for the docking. The Hermes visualizer in the GOLD Suite was used to further prepare the metal complexes and the receptors for docking. The optimized DPPD and 4,4'-bipyridine ligands and also cif file of the complex 3 were used for docking studies. The region of interest used for Gold docking was defined as all the protein residues within the 6 Å of the reference ligand "A" that accompanied the downloaded protein. All free water molecules in the structure of the proteins were deleted before docking. Default

**Table 2**  
Selected bond length (Å) and angles (°) for complexes 1–4 and Z-HMPP with standard deviations in parentheses.

	Z-HMPP	1	2	3	4	
Distances	C7 – O1	1.287(2)	Cd1 – O1	2.241(5)	Cd1 – O1	2.241
	C9 – O2	1.295(2)	Cd1 – O2	2.193(4)	Cd1 – O2	2.240
	C3 – O3	1.352(2)	Cd1 – O3	2.264(4)	Cd1 – N1	2.370
	C13 – O4	1.361(2)	Cd1 – O4	2.569(5)	Cd1 – N2	
	C6 – 7	1.465(2)	Cd1 – O4	2.310(5)	Zn1A – O1A	2.002(2)
	C9 – C10	1.463(2)	Cd1 – N1	2.302(5)	Zn1A – N1A	2.058(3)
Angles	C4 – C3 – O3	116.2(1)	O1 – Cd1 – O2	82.5(2)	O1 – Cd1 – O2	81.1
	C6 – C7 – O1	116.5(1)	O2 – Cd1 – O3	141.5(2)	O2 – Cd1 – N2	95.9
	C8 – C9 – O2	119.4(1)	O3 – Cd1 – O4	52.8(2)	N2 – Cd1 – N1	96.3
	C12 – C13 – O4	124.9(2)	O4 – Cd1 – O4	73.5(2)	N1 – Cd1 – O1	94.2
			O4 – Cd1 – N1	89.5(2)		
			N1 – Cd1 – O1	88.3(2)	O1A – Zn1A – O2A	87.2(1)
				O2A – Zn1A – O3A	165.5(1)	
				O3A – Zn1A – O4A	89.4(1)	
				O4A – Zn1A – N1A	100.9(1)	
				N1A – Zn1A – O2A	94.9(1)	

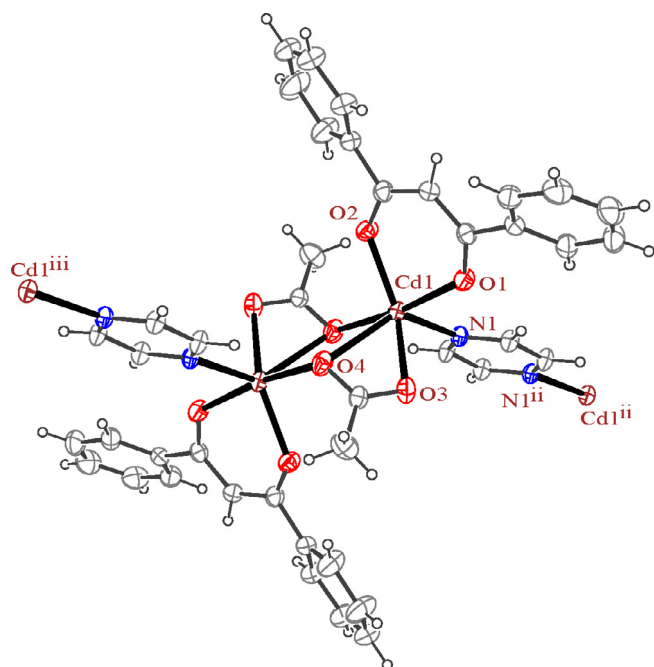


Fig. 1. ORTEP diagram of the excerpt from coordination polymer structure of **1**. The ellipsoids are drawn at the 35% probability level.

values of all other parameters were used and the complexes were submitted to 10 genetic algorithm runs using the GOLDScore fitness function.

### 3. Results and discussion

Reaction between cadmium(II) acetate with HDPPD/pyrazine, HDPPD/4,4'-bipyridine and HDPPD/DPP mixtures in branched tubes provide 1D coordination polymers **1**, **2** and **4**, respectively. In similar reaction, the zinc(II) acetate was reacted with HDPPD/4,4'-bipyridine mixture and observed that the zinc atom preferred a binuclear structure respect to the polymeric backbone. The complexes are air-stable and soluble in DMSO.

#### 3.1. Spectroscopic characterization

In the IR spectra of the complexes **1–4**, the relatively weak absorption bands at about 3100 and 3050  $\text{cm}^{-1}$  are due to the C–H modes of the aromatic rings and  $\beta$ -diketone unit, respectively. For complexes **1** and **4**, frequencies near the 2950  $\text{cm}^{-1}$  are related to the aliphatic moieties (acetate in **1** and propane in **4**) in their structures. In all the spectra of complexes, there are three bands corresponding to the anionic  $\beta$ -diketone unit of the DPPD including 1550–1600  $\text{cm}^{-1}$  due to the  $\nu$  (C=C) coupled with  $\nu$  (C=O), 1500–1550 to the  $\nu$  (C=O) coupled with  $\nu$  (C=C) and near 1450  $\text{cm}^{-1}$  to the  $\delta$  (C–H) coupled with  $\nu$  (C=C) [64]. The neutral free HDPPD has a band 1655  $\text{cm}^{-1}$  corresponding to the carbonyl unit of the keto form [65] which is shifted to lower frequencies upon coordination due to the deprotonation of the  $\beta$ -diketone unit. The pyridine and pyrazine rings of the linkage ligands are noted in the FT-IR spectra of complexes in the region of 1500–1600  $\text{cm}^{-1}$  owing to the  $\nu$  (C=N)<sub>ar</sub> [66].

In the FT-IR spectrum of **1**, three bands at 1543, 1434 and 674  $\text{cm}^{-1}$  were assigned to the  $\nu_{\text{as}}$  (COO),  $\nu_{\text{s}}$  (COO) and  $\delta$  (OCO) respectively [67], confirming the presence of the acetate unit in this complex. The differences between asymmetric ( $\nu_{\text{as}}$ ) and symmetric ( $\nu_{\text{s}}$ ) stretching of the acetate group ( $\Delta$ ) can reveal its coordination type. In monodentate complexes,  $\Delta$  values are much greater than the acetate salt (164  $\text{cm}^{-1}$ ) while in bidentate complexes these values are significantly less than the

acetate salt [68,69]. The  $\Delta$  value for **1** is 109  $\text{cm}^{-1}$  which is corresponding to the bidentate acetate ligand.

The  $^1\text{H}$  NMR spectrum of the complex **1** (Supplementary Materials) revealed that aromatic (7.40–8.64 ppm), aliphatic (1.82) and alkene (6.54 ppm) moieties of this structure. The hydrogen atoms of the acetate and pyrazine ligands are observed at the highest and lowest magnetic field, respectively. A singlet at the 6.54 ppm with integral of 1 is characteristic peak of the anionic  $\beta$ -diketone unit of the DPPD. By comparing the intensity of this signal with acetate and pyrazine ligands, the structure of the complex can be determined. Based on the intensity ratio of 3:1:2 respectively for acetate,  $\beta$ -diketone unit and pyrazine ligand, we can conclude that the stoichiometry of 1 mol acetate, 1 mol DPPD and 0.5 mol pyrazine per each cadmium atom in the structure of the complex **1** which is confirmed by the X-ray analysis.

The  $^1\text{H}$  NMR spectrum of **2** revealed that a mixed ligands structure. The sum of the integral numbers of all signals related to the DPPD is 22 (each DPPD has 11 hydrogen atoms) and 4,4'-bipyridine is 8 (each 4,4'-bipyridine has 8 hydrogen atoms), confirming the stoichiometry of 2:1 for DPPD:4,4'-bipy. Two doublet signals for 4,4'-bipyridine ligand reveal a symmetrical bridging coordination mode. The integral numbers in the  $^1\text{H}$  NMR spectrum of **3** supports a different stoichiometry to **2**. In this complex, the stoichiometry of DPPD:4,4'-bipy is 2:0.5 which can be adopted only with the binuclear structure in which the 4,4'-bipyridine coordinates as symmetrical bridged ligand between two zinc atoms.

In the  $^1\text{H}$  NMR spectrum of the complex **4**, eight hydrogen atoms of the two pyridinic rings of the DPP ligand appear as two sets of doublet signals which support the symmetrical bridging behaviour of this ligand. Also sum of the integral numbers of the DPPD and DPP ligands confirms the ratio of 2:1, respectively, thus a polymeric structure is anticipated for the complex **4**.

The FT-IR and  $^1\text{H}$  NMR spectra of *Z*-HMPP reveal a  $\beta$ -diketone ligand in its enolic form. In the FT-IR spectrum of this compound, the frequencies at 1604, 1545 and 1303  $\text{cm}^{-1}$  correspond to the  $\nu$  (C=C),  $\nu$  (C=O) and  $\nu$  (C–O) which are characteristics of the enolic form [70]. Also singlet signals of the 7.51 and 7.17 ppm in the  $^1\text{H}$  NMR spectrum were assigned to the hydrogen atoms methylene and alcoholic groups of the  $\beta$ -diketone moiety in agree with its enolic structure.

#### 3.2. Description of the crystal structures

##### 3.2.1. Crystal structures of $\{(\mu\text{-OAc})(\text{DPPD})\text{Cd}(\mu\text{-PYZ})\text{Cd}(\text{DPPD})(\mu\text{-OAc})\}_n$ (**1**)

In the crystal structure of **1** (Fig. 1), the cadmium atom is coordinated by three oxygen atoms of two acetate ligands, two oxygen atoms of one DPPD and one nitrogen atom of a pyrazine ligand with distorted octahedral geometry. Among the five Cd–O bond lengths, the bond lengths of DPPD ligand are shorter than the others. The complex has one center of inversion on the center of pyrazine ring and  $C_i$  symmetry. This structure is a 1D asymmetric zigzag-coordination polymer (Figs. S1 and S5, Supplementary Materials) [71] of cadmium containing two types of bridges, one Cd-pyrazine-Cd bridge and two Cd-acetate-Cd bridges. The DPPD ligand does not participate in the polymeric backbone but completes the octahedral geometry around the cadmium atom (Fig. S5, Supplementary Materials). To compare the coordination mode of the acetate ligand in **1** with published analogues, a structural survey was carried out and results are presented in Table S3 (Supplementary Materials). These data revealed that seven different coordination modes have been reported for cadmium complexes containing the acetate ligand. Among these coordination modes, the “(O,O)” mode (Fig. 2) is the most observed ones (54%) in which the acetate unit acts as  $\text{O}_2$ -donor and forms one four-membered chelate ring. The observed mode in **1** is “(O,  $\mu$ -O)” which is the second most common in the CSD analogues (24%). In another comparison, the percentage of bridged and non-bridged structures was calculated. These data revealed that the acetate unit commonly forms a non-bridged structure (71%). In mostly cases this ligand forms a chelate ring with cadmium atom (81%).

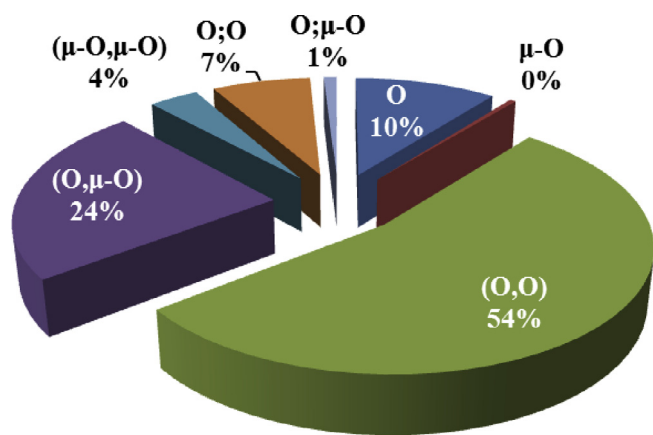


Fig. 2. Pie chart, the percentage of different coordination modes of the acetato ligand among the complexes of cadmium.

Each DPPD ligand acts as bidentate and forms a six-membered planar chelate ring (with r.m.s value of 0.075 Å for O1 atom). Two phenyl groups are not coplanar with the chelate ring and are bended from this plane with the average bending angles of 39.07°. For study of the bond lengths and angles variation of the HDPPD after coordination to the cadmium atom, the geometrical parameters of free ligand (Scheme S2, Supplementary Materials) [72] were compared with the **1**. After coordination, the C–C–C bond angle of the β-diketone moiety (127.20°) is increased about 6.78° and the bending angle of the phenyl groups respect to the plane through the β-diketone moiety (39.07°) is increased about 28.2° (these values for free ligand are 120.42° and 10.86°, respectively).

The pyrazine ligand in the complex of **1** connects two cadmium atoms. These atoms are not lie on the mean plane through the pyrazine ring; one cadmium atom places above this plane and another under it with distance of 0.229 Å.

### 3.2.2. Crystal structure of $\{Cd(\mu-4,4'-Bipy)(DPPD)_2\}_n$ (**2**)

In the crystal structure of **2** (Fig. 3), the cadmium atom is coordinated by two O-donor DPPD and two 4,4'-bipyridine with slightly distorted octahedral geometry (Fig. S6, Supplementary Materials). The 4,4'-bipyridine ligand connects two cadmium atoms to form 1D linear-coordination polymer [71]. The Cd–O bond lengths are shorter than the Cd–N bond lengths (Table 2) and these two bond lengths are comparable with the CSD average for complexes containing the unit (Scheme S3(a), Supplementary Materials).

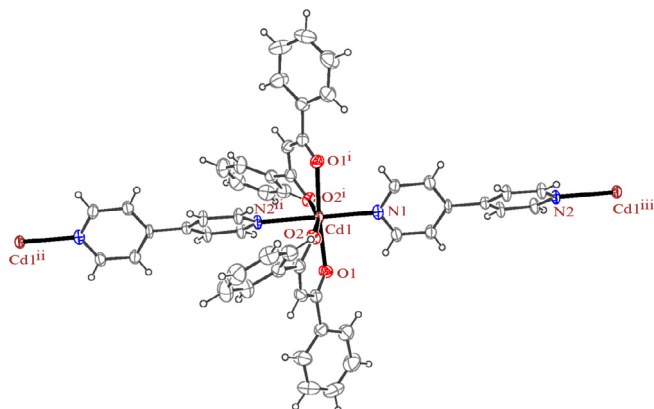


Fig. 3. ORTEP diagram of the excerpt from coordination polymer structure of **2**. The ellipsoids are drawn at the 35% probability level.

In this structure, the six-membered chelate ring formed by DPPD is not planar (with r.m.s value of 0.265 Å for O2 atom). The average of bending angles of two phenyl groups from the chelate ring is 41.85° which is higher than that of the complex **1**. These observations (non-planar chelate ring and increasing the bending angle of phenyl groups) can be attributed to the increasing the C–C–C bond angle of the β-diketone moiety about 0.73° respect to the **1**.

The two pyridine rings of the 4,4'-bipyridine ligand are not coplanar and dihedral angle between their planes is 41.39° which is higher than the CSD average for bridged 4,4'-bipyridine between two cadmium atom (17.07°). This angle in the free ligand [73] is 26.69° (this value is the average of dihedral angles for two independent structures [73]).

### 3.2.3. Crystal structure of $[(DPPD)_2Zn(\mu-4,4'-Bipy)Zn(DPPD)_2]$ (**3**)

In the crystal structure of the complex **3** (Fig. 4), there are two independent binuclear zinc complexes with slightly difference in geometrical parameters. The zinc atom is coordinated by one nitrogen atom of a 4,4'-bipyridine ligand and four oxygen atoms of two DPPD ligand with coordination number of five. A penta-coordinate geometry of **3**, may adopt either a square pyramidal or a trigonal bipyramidal structure which is determined by applying the formula of Addison et al. [74,75]. The angular structural parameter,  $\tau$  ( $\tau = (\beta - \alpha)/60$ , where  $\alpha$  and  $\beta$  are the two largest angles at the zinc atom with  $\beta \geq \alpha$ ), was calculated to be 0.31 and 0.30, respectively for Zn1A and Zn1B indicating a distorted square-pyramidal geometry (Fig. S7, Supplementary Materials). Studying the CSD database for the base presented in Scheme S3(b), Supplementary Materials, revealed that the coordinated bond lengths of **3** are comparable with the CSD average (Zn–N, 2.057; Zn–O, 2.006) and in all complexes the average of all Zn–O bond lengths is shorter than the Zn–N bond lengths.

The coordinated DPPD ligand forms a non-planar six-membered chelate ring around the zinc atom. The average of dihedral angles between phenyl groups and chelate ring plane is 14.57° which is lower than in **1** and **2** which can be related to the lowest value of the C–C–C bond angle in **3** (126.00°) respect to the **1** and **2**.

The dihedral angle between two pyridine rings of the 4,4'-bipyridine ligand is 0.00°, showing that the planar coordination behavior of this ligand toward zinc atom. This value for the CSD analogues is 14.94° which is lower than that of the cadmium analogues (17.07°).

### 3.2.4. Crystal structure of $\{Cd(\mu-DPP)(DPPD)_2\}_n$ (**4**)

X-ray analysis of the complex **4** reveals (Fig. 5) 1D symmetric linear-coordination polymer; extending by bridging 1,3-di(pyridin-4-yl)propane between cadmium atoms. In this structure, the cadmium atom by coordination of four oxygen atoms of two O<sub>2</sub>-donor DPPD and two nitrogen atoms of two 1,3-di(pyridin-4-yl)propane has a octahedral geometry (Fig. S8, Supplementary Materials). The Cd–O bond lengths (2.241 Å) are shorter than the Cd–N (2.370 Å) and these two bond lengths are comparable with the CSD average (Scheme S3(a), Supplementary Materials).

The dihedral angles average between phenyl groups with the planar chelate ring of DPPD (with r.m.s value of 0.029 Å for C7 atom) is 19.89° which is higher than that of the free ligand and can be attributed to the increasing the C–C–C bond angle of coordinated DPPD (Table 3). The dihedral angle between two pyridine rings of the 1,3-di(pyridin-4-yl)propane ligand is 79.87°.

### 3.2.5. Crystal structure of (Z)-3-hydroxy-1,3-bis(4-methoxyphenyl)prop-2-en-1-one (Z-HMPP)

X-ray analysis of the (Z)-3-hydroxy-1,3-bis(4-methoxyphenyl)prop-2-en-1-one revealed a Z conformation and enolic form of this ligand (Fig. 6). These types of the compounds have two tautomeric forms including enol and keto. Study of the all CSD structures containing β-diketone unit (the structures in which the β-diketone unit is fused to a ring were omitted) revealed that the enol form (292 hits, 88%) is more common than the keto form (41 hits, 12%) as observed in the Z-HMPP.

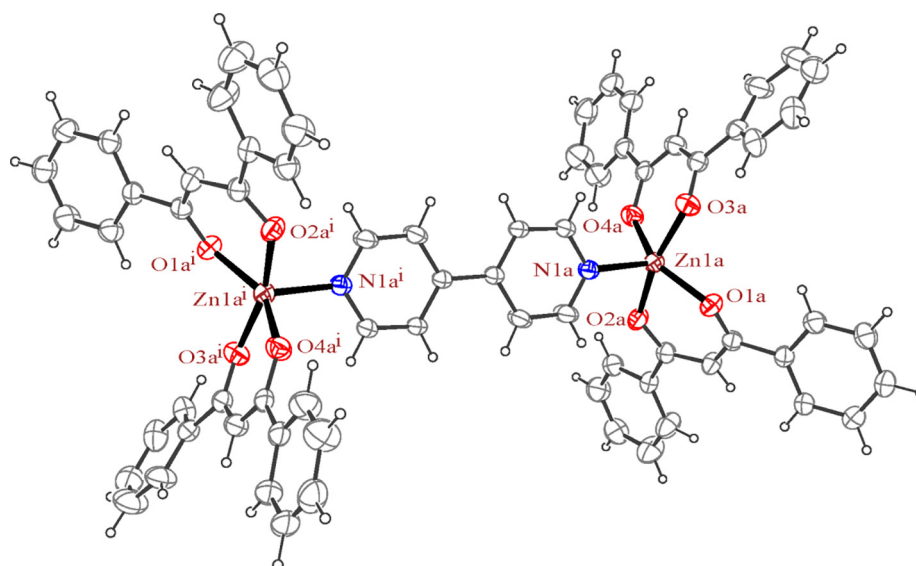


Fig. 4. ORTEP diagram of the molecular structure of **3**. The ellipsoids are drawn at the 25% probability level.

The bond lengths average of the  $\beta$ -diketone unit were extracted and presented in [Scheme S4, Supplementary Materials](#). The data revealed that the C=O bond length is the shortest bond in this unit. The hydrogen atom of the hydroxyl group along with the oxygen atom of the side carbonyl group form a planar six-membered hydrogen bonding ring (with r.m.s value of 0.039 Å for H1 atom). The phenyl groups of the ligand are almost coplanar with this ring with the dihedral angle average of 3.87°.

### 3.2.6. Crystal network interactions

In the crystal network of compounds ([Figs. S5–S9, Supplementary Materials](#)) intermolecular C–H $\cdots$ O, and C–H $\cdots$ C (except in **1** and Z-HMPP) also intramolecular O–H $\cdots$ O (Z-HMPP) hydrogen bonds appear between adjacent complexes. In this way the carbon and oxygen atoms participate in hydrogen bonding as proton donors and acceptors at the same time. In addition to the hydrogen bonds, the crystal networks of the compounds are further stabilized by  $\pi$ – $\pi$  stacking interactions between aromatic rings [76,77] of the adjacent ligands ([Figs. S5–S9, Supplementary Materials](#)). In the crystal network of **1** ([Fig. S5, Supplementary Materials](#)), there are  $\pi$ – $\pi$  stacking interaction between the pyrazine and phenyl group of the DPPD which has the shortest centroid-centroid distance among the all compounds and strongest ones ([Table S1, Supplementary Materials](#)). Similar interaction is appeared between phenyl ring of the DPPD and pyridine ring of the 4,4'-bipyridine ligands. Although the complexes **2** and **3** have similar ligands but

**Table 3**

Differences ( $\Delta$ ) of the C–C and C–O bond lengths and central C–C–C bond angle of the  $\beta$ -diketone unit and dihedral angles average between phenyl groups with the mean plan through the chelate ring of the coordinated DPPD in the complexes **1–4** and HDPPD.

	$\Delta$ (C–C)	$\Delta$ (C–O)	C–C–C	Dihedral Angle
HDPPD	0.027	0.025	120.42°	10.86°
<b>1</b>	0.005	0.008	127.20	39.07
<b>2</b>	0.018	0.000	127.93	41.85°
<b>3</b>	0.005	0.006	126.00	14.57°
<b>4</b>	0.000	0.007	127.03	19.89

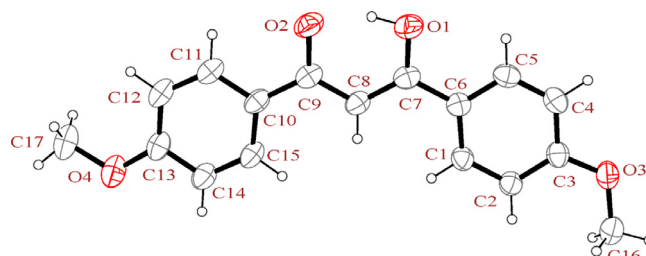


Fig. 6. ORTEP diagram of the molecular structure of Z-HMPP. The ellipsoids are drawn at the 35% probability level.

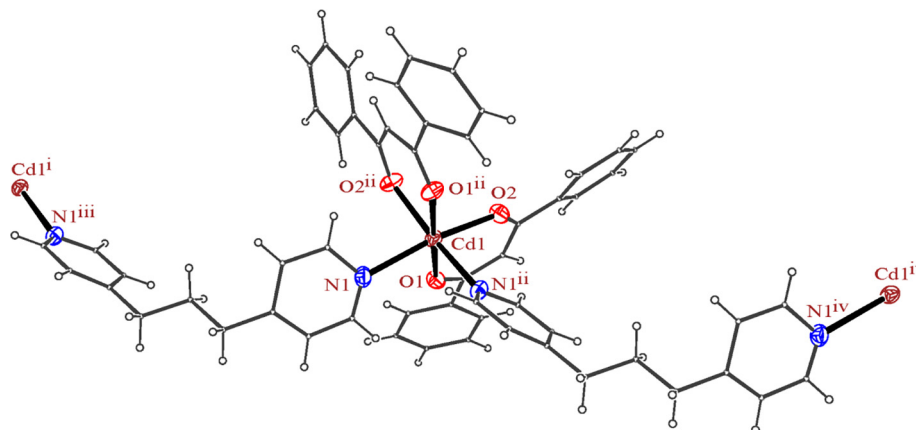


Fig. 5. ORTEP diagram of the excerpt from coordination polymer structure of **4**. The ellipsoids are drawn at the 35% probability level.



**Table 4**The calculated fitness values for the complex **3**, 4,4'-bipyridine and DPPD.

Top II	TS	TrxR	RNR	rHA	HDAC7	DNA-Gyrase	CatB	BRAF-Kinase	
32.44	32.93	36.76	32.75	33.95	38.16	36.27	24.02	33.85	4,4'-Bipyridine
41.77	39.88	45.58	36.98	43.64	45.11	39.68	28.70	42.73	DPPD
0.00	81.66	63.56	79.60	-185.66	0.00	0.00	0.00	0.00	Complex <b>3</b>

### 3.4. Docking studies

For predicting and comparison the biological activities of the complex **3**<sup>2</sup> and its ligands (4,4'-bipyridine and DPPD), interactions of these compounds with nine macromolecule receptors using Gold [63] docking software were studied. The Gold docking results are reported in terms of the values of fitness which means the higher the fitness the better the docked interaction of the compounds [53]. The results of the docking presented in this work is the best binding results out of the favorably ten predicted by Gold.

The general features from the Gold docking prediction (Table 4) show that all studied structures can be considered as biologically active compounds (Fig. S9 and S10, S11 Supplementary). The best predicted targets for the 4,4'-bipyridine and DPPD ligands is HDAC7 and TrxR, respectively, while for the studied complex **3** is TS. The GOLDScore fitness values of the complex **3** revealed that this complex can interact selectively with three biomacromolecules of RNR, TrxR and TS among the nine biomacromolecules. Also complex **3** can interacted with the mentioned proteins better than the free ligands of 4,4'-bipyridine and DPPD. In other cases (other biomacromolecules than RNR, TrxR and TS) two free ligands are biologically active while after coordination to zinc they become inactive. A fitness value comparison between 4,4'-bipyridine and DPPD could allow to conclude that the DPPD has better binding ability toward proteins than the 4,4'-bipyridine.

## 4. Conclusion

Compounds of  $\{(\mu\text{-OAc})(\text{DPPD})\text{Cd}(\mu\text{-PYZ})\text{Cd}(\text{DPPD})(\mu\text{-OAc})\}_n$  (**1**); HDPPD: 1,3-diphenylpropane-1,3-dione,  $\{\text{Cd}(\mu\text{-4,4'-Bipy})(\text{DPPD})_2\}_n$  (**2**),  $[(\text{DPPD})_2\text{Zn}(\mu\text{-4,4'-Bipy})\text{Zn}(\text{DPPD})_2]$  (**3**),  $\{\text{Cd}(\mu\text{-DPP})(\text{DPPD})_2\}_n$  (**4**); DPP: 1,3-di(pyridin-4-yl)propane and (*Z*)-3-hydroxy-1,3-bis(4-methoxyphenyl)prop-2-en-1-one (*Z*-HMPP) were prepared; their spectral (IR, <sup>1</sup>H NMR) and structural (single crystal X-ray diffraction) properties were investigated. Among these structures, the cadmium complexes **1**, **2** and **4** have 1D polymeric structure with octahedral geometry containing *N*-donor ligands as linkers (in **1**, there are two types of linker ligands, *N*-donor and *O*-donor). The complex **3** has binuclear structure and distorted square-pyramidal geometry at the zinc atom. Among the different coordination modes of the acetate ligand which is coordinated to the cadmium atom, the "(O,O)" mode is the most observed ones (54%). In all complexes, the bond angle of the  $\beta$ -diketone moiety and dihedral angles between phenyl groups with the mean plan through the chelate ring of this moiety is increased with respect to the free ligand. In addition to the hydrogen bonds in the crystal network of the complexes, there are  $\pi$ - $\pi$  stacking interactions between aromatic rings, showing the high ability of these molecules to interact with neighboring units and making them good choice to docking studies. The docking studies on the 4,4'-bipyridine, DPPD and complex **3** revealed that the these compounds might be biologically active by interacting with the nine biomacromolecules (BRAF kinase, CatB, DNA gyrase, HDAC7, rHA, RNR, TrxR, TS and Top II). The best predicted targets for the 4,4'-bipyridine, DPPD and complex **3** is HDAC7, TrxR and TS, respectively. Also **3** can interact selectively with three biomacromolecules of RNR, TrxR and TS. Based on the calculated

<sup>2</sup> The compounds containing cadmium atom are not good choice for biological active compounds.

fitness values of titled compounds, we suggest that studying anticancer activities of these compounds could be interesting. The PSS<sup>5</sup> parameter for three complexes **1**, **2** and **4** were calculated to be -2274, -2118 and -2000, confirming that by growing the chain of complex **1** the thermodynamic stability of it is increased higher than the others. The NBO analysis of the optimized complex **3** revealed that the hydrogen and carbon atoms of two coordinated ligands act as electron donor and decrease the charge of the zinc atom.

## Appendix A. Supplementary data

Supplementary data associated with this article can be found, in the online version, at <https://doi.org/10.1016/j.ica.2018.07.014>.

## References

- [1] H.-Y. Wang, L. Cui, J.-Z. Xie, C.F. Leong, D.M. D'Alessandro, J.-L. Zuo, *Coord. Chem. Rev.* 345 (2017) 342–361.
- [2] H. Yao, F. Zhang, G. Zhang, H. Luo, L. Liu, M. Shen, Y. Yang, A novel two-dimensional coordination polymer-polypyrrole hybrid material as a high-performance electrode for flexible supercapacitor, *Chem. Eng. J.* 334 (2018) 2547–2557.
- [3] S. Kitagawa, *Angew. Chem. Int. Ed.* 54 (2015) 10686–10687.
- [4] J. Goldsmith, A.G. Wong-Foy, M.J. Cafarella, D.J. Siegel, *Chem. Mater.* 25 (2013) 3373–3382.
- [5] D. Alezi, Y. Belmabkhout, M. Suyetin, P.M. Bhatt, L.J. Weseliński, V. Solovyeva, K. Adil, I. Spanopoulos, P.N. Trikalitis, A.-H. Emwas, M. Eddaoudi, *J. Am. Chem. Soc.* 137 (2015) 13308–13318.
- [6] C.V. McGuire, R.S. Forgan, *Chem. Comm.* 51 (2015) 5199–5217.
- [7] C.R. Pfeiffer, D.A. Fowler, J.L. Atwood, *CrystEngComm* 17 (2015) 4475–4485.
- [8] M. Fernandez, A.S. Barnard, *A.C.S. Comb. Sci.* 18 (2016) 243–252.
- [9] C. Pettinari, F. Marchetti, N. Mosca, G. Tosi, A. Drozdov, *Polym. Int.* 66 (2017) 731–744.
- [10] R. Feng, Y.-Y. Jia, Z.-Y. Li, Z. Chang, X.-H. Bu, *Chemical Science* 9 (2018) 950–955.
- [11] Y. Cui, F. Zhu, B. Chen, G. Qian, *Chem. Comm.* 51 (2015) 7420–7431.
- [12] Z. Hu, B.J. Deibert, J. Li, *Chem. Soc. Rev.* 43 (2014) 5815–5840.
- [13] D. Zhao, Y. Cui, Y. Yang, G. Qian, *CrystEngComm* 18 (2016) 3746–3759.
- [14] D. Ma, B. Li, X. Zhou, Q. Zhou, K. Liu, G. Zeng, G. Li, Z. Shi, S. Feng, *Chem. Comm.* 49 (2013) 8964–8966.
- [15] P. Kumar, A. Deep, K.-H. Kim, *Trends Anal. Chem.* 73 (2015) 39–53.
- [16] M.Y. Masoomi, A. Morsali, P.C. Junk, J. Wang, Ultrasonic assisted synthesis of two new coordination polymers and their applications as precursors for preparation of nano-materials, *Ultrason. Sonochem.* 34 (2017) 984–992.
- [17] M. Kurmoo, *Chem. Soc. Rev.* 38 (2009) 1353–1379.
- [18] J.S. Miller, *Dalton Trans.* (2006) 2742–2749.
- [19] D. Tiana, C.H. Hendon, A. Walsh, *Chem. Comm.* 50 (2014) 13990–13993.
- [20] P. Kar, R. Haldar, C.J. Gómez-García, A. Ghosh, *Inorg. Chem.* 51 (2012) 4265–4273.
- [21] X.-Q. Wu, M.-L. Han, G.-W. Xu, B. Liu, D.-S. Li, J. Zhang, *Inorg. Chem. Commun.* 58 (2015) 60–63.
- [22] Y. Cui, Y. Yue, G. Qian, B. Chen, *Chem. Rev.* 112 (2012) 1126–1162.
- [23] D.F. Sava Gallis, L.E.S. Rohwer, M.A. Rodriguez, T.M. Nenoff, *Chem. Mater.* 26 (2014) 2943–2951.
- [24] Z.-L. Fang, X.-Y. Wu, R.-M. Yu, C.-Z. Lu, *CrystEngComm* 16 (2014) 8769–8776.
- [25] C.A. Bauer, T.V. Timofeeva, T.B. Settersten, B.D. Patterson, V.H. Liu, B.A. Simmons, M.D. Allendorf, *J. Am. Chem. Soc.* 129 (2007) 7136–7144.
- [26] J. Liu, L. Chen, H. Cui, J. Zhang, L. Zhang, C.-Y. Su, *Chem. Soc. Rev.* 43 (2014) 6011–6061.
- [27] S. Kitagawa, R. Kitaura, S.-I. Noro, *Angew. Chem. Int. Ed.* 43 (2004) 2334–2375.
- [28] J. Gascon, A. Corma, F. Kapteijn, F.X. Llabrés i Xamena, *ACS Catal.* 4 (2014) 361–378.
- [29] A.H. Chughtai, N. Ahmad, H.A. Younus, A. Laypkov, F. Verpoort, *Chem. Soc. Rev.* 44 (2015) 6804–6849.
- [30] X. Zhang, M. Cui, R. Zhou, C. Chen, G. Zhang, *Macromol. Rapid Commun.* 35 (2014) 566–573.
- [31] S. Schwieger, R. Herzog, C. Wagner, D. Steinborn, *J. Organomet. Chem.* 694 (2009) 3548–3558.
- [32] C.-J. Xu, B.-G. Li, J.-T. Wan, Z.-Y. Bu, *J. Lumin.* 131 (2011) 1566–1570.
- [33] K. Buczek, M. Karbowski, *J. Lumin.* 136 (2013) 130–140.
- [34] Z. Ahmed, R.E. Aderne, J. Kai, J.A.L.C. Resende, H.I. Padilla-Chavarria, M. Cremona, *RSC Adv.* 7 (2017) 18239–18251.
- [35] Z. Ahmed, R.E. Aderne, J. Kai, H.I.P. Chavarria, M. Cremona, *Thin Solid Films* 620

- (2016) 34–42.
- [36] J.C.-H. Chan, W.H. Lam, H.-L. Wong, N. Zhu, W.-T. Wong, V.W.-W. Yam, *J. Am. Chem. Soc.* 133 (2011) 12690–12705.
- [37] R. Yoshii, A. Hirose, K. Tanaka, Y. Chujo, *J. Am. Chem. Soc.* 136 (2014) 18131–18139.
- [38] T. Butler, W.A. Morris, J. Samonina-Kosicka, C.L. Fraser, *ACS Appl. Mater. Interfaces* 8 (2016) 1242–1251.
- [39] G. Zhang, G.M. Palmer, M.W. Dewhurst, C.L. Fraser, *Nat. Mater.* 8 (2009) 747.
- [40] J. Samonina-Kosicka, C.A. DeRosa, W.A. Morris, Z. Fan, C.L. Fraser, *Macromol.* 47 (2014) 3736–3746.
- [41] S. Mukherjee, P. Thilagar, *Chem. Comm.* 51 (2015) 10988–11003.
- [42] M.N. Kopylovich, Y.Y. Karabach, K.T. Mahmudov, M. Haukka, A.M. Kirillov, P.J. Figiel, A.J.L. Pombeiro, *Crystal Growth & Design* 11 (2011) 4247–4252.
- [43] K.T. Mahmudov, M.F.C. Guedes da Silva, A.M. Kirillov, M.N. Kopylovich, A. Mizar, A.J.L. Pombeiro, *Crystal Growth & Design* 13 (2013) 5076–5084.
- [44] G.D. Diana, P.M. Carabateas, R.E. Johnson, G.L. Williams, F. Pancic, J.C. Collins, *J. Med. Chem.* 21 (1978) 889–894.
- [45] R.K. Maheshwari, A.K. Singh, J. Gaddipati, R.C. Srimal, *Life Sci.* 78 (2006) 2081–2087.
- [46] H. Foks, D. Pancechowska-Ksepko, A. Kędzia, Z. Zwolska, M. Janowiec, E. Augustynowicz-Kopeć, *Il Farmaco* 60 (2005) 513–517.
- [47] M.M. Ghorab, A.Y. Hassan, *Phosphorus Sulfur Silicon Relat. Elem.* 141 (1998) 251–261.
- [48] R. Chen, C.-S. Liu, H. Zhang, Y. Guo, X.-H. Bu, M. Yang, *J. Inorg. Biochem.* 101 (2007) 412–421.
- [49] H. Zhang, C.-S. Liu, X.-H. Bu, M. Yang, *J. Inorg. Biochem.* 99 (2005) 1119–1125.
- [50] M. Dardenne, J.M. Pléau, B. Nabarra, P. Lefrancier, M. Derrien, J. Choay, J.F. Bach, *Proc. Natl. Acad. Sci.* 79 (1982) 5370–5373.
- [51] O. Birmingham-McDonogh, E.B. Gralla, J.S. Valentine, *Proc. Natl. Acad. Sci.* 85 (1988) 4789–4793.
- [52] A.H. Shankar, A.S. Prasad, *Am. J. Clin. Nutr.* 68 (1998) 447S–463S.
- [53] A.A. Adeniyi, P.A. Ajibade, *Molecules* 18 (2013) 3760–3778.
- [54] G. Mahmoudi, A. Morsali, A.D. Hunter, M. Zeller, *CrystEngComm* 9 (2007) 704–714.
- [55] F. Marandi, F. Amoopour, I. Pantenburg, G. Meyer, *J. Mol. Struct.* 973 (2010) 124–129.
- [56] APEX-II, Bruker Advanced X-ray Solutions (version 1-0), Bruker AXS Inc, Madison, Wisconsin (USA), 2009.
- [57] G. Sheldrick, *Acta crystallographica. Section A, Foundations of crystallography*, A64 (2008) 112–122.
- [58] L.J. Farrugia, *J. Appl. Crystallogr.* 30 (1997) 565.
- [59] M.N. Burnett, C.K. Johnson, Ortep-III, Report ORNL-6895, Oak Ridge National Laboratory, Oak Ridge, Tennessee, U.S., 1996.
- [60] G. Bergerhof, M. Berndt, K. Brandenburg, *J. Res. Nat. Inst. Stand. Technol.* 101 (1996) 221–225.
- [61] M.J. Frisch, G.W. Trucks, H.B. Schlegel, G.E. Scuseria, M.A. Robb, J.R. Cheeseman, G. Scalmani, V. Barone, B. Mennucci, G.A. Petersson, H. Nakatsuji, M. Caricato, X. Li, H.P. Hratchian, A.F. Izmaylov, J. Bloino, G. Zheng, J.L. Sonnenberg, M. Hada, M. Ehara, K. Toyota, R. Fukuda, J. Hasegawa, M. Ishida, T. Nakajima, Y. Honda, O. Kitao, H. Nakai, T. Vreven, J.A. Montgomery Jr., J.E. Peralta, F. Ogliaro, M.J. Bearpark, J. Heyd, E.N. Brothers, K.N. Kudin, V.N. Staroverov, R. Kobayashi, J. Normand, K. Raghavachari, A.P. Rendell, J.C. Burant, S.S. Iyengar, J. Tomasi, M. Cossi, N. Rega, N.J. Millam, M. Klene, J.E. Knox, J.B. Cross, V. Bakken, C. Adamo, J. Jaramillo, R. Gomperts, R.E. Stratmann, O. Yazyev, A.J. Austin, R. Cammi, C. Pomelli, J.W. Ochterski, R.L. Martin, K. Morokuma, V.G. Zakrzewski, G.A. Voth, P. Salvador, J.J. Dannenberg, S. Dapprich, A.D. Daniels, Ö. Farkas, J.B. Foresman, J.V. Ortiz, J. Cioslowski, D.J. Fox, Gaussian 09, in, Gaussian Inc, Wallingford, CT, USA, 2009.
- [62] J.P. Perdew, *Phys. Rev. B* 33 (1986) 8822–8824.
- [63] G. Jones, P. Willett, R.C. Glen, A.R. Leach, R. Taylor, *J. Mol. Biol.* 267 (1997) 727–748.
- [64] K. Nakamoto, in: 6 (Ed.), *Infrared and raman spectra of inorganic and coordination compounds 2009* John Wiley Hoboken 259 260.
- [65] F. Marandi, *J. Mol. Struct.* 1059 (2014) 75–80.
- [66] M. Hakimi, Z. Mardani, K. Moeini, E. Schuh, F. Mohr, *Z. Naturforsch.*, 68b (2013) 267.
- [67] F. Marandi, K. Moeini, A. Rudbari Hadi, *Z. Naturforsch.*, 71b (2016) 959.
- [68] K. Nakamoto, in: 6 (Ed.) *Infrared and raman spectra of inorganic and coordination compounds*, John Wiley, Hoboken, 2009, pp. 232.
- [69] M. Hakimi, K. Moeini, Z. Mardani, F. Khorrami, *J. Korean Chem. Soc.* 57 (2013) 352–356.
- [70] Y. Akama, A. Tong, *Microchem. J.* 53 (1996) 34–41.
- [71] M. Sánchez-Serratos, J. Raziel Álvarez, E. González-Zamora, I.A. Ibarra, *J. Mex. Chem. Soc.* 60 (2017).
- [72] D. Williams, *Acta Crystallogr., Sect. A: Found. Crystallogr.* 21 (1966) 340–349.
- [73] N.M. Boag, K.M. Coward, A.C. Jones, M.E. Pemble, J.R. Thompson, *Acta Crystallogr., Sect. A: Found. Crystallogr.* C55 (1999) 672–674.
- [74] A.W. Addison, T. Rao, J. Reedijk, J.V. Rijn, G. Verschoor, *Dalton Trans.* (1984) 1349.
- [75] M. Hakimi, Z. Mardani, K. Moeini, F. Mohr, *Polyhedron* 102 (2015) 569.
- [76] F. Marandi, K. Moeini, B. Mostafazadeh, H. Krautscheid, *Polyhedron* 133 (2017) 146–154.
- [77] F. Marandi, K. Moeini, S. Ghasemzadeh, Z. Mardani, C.K. Quah, W.-S. Loh, *J. Mol. Struct.* 1149 (2017) 92–98.
- [78] C.F. Macrae, I.J. Bruno, J.A. Chisholm, P.R. Edgington, P. McCabe, E. Pidcock, L. Rodriguez-Monge, R. Taylor, J. Van De Streek, P.A. Wood, *J. Appl. Crystallogr.* 41 (2008) 466–470.
- [79] A. Gavezzotti, G. Filippini, *J. Phys. Chem.* 98 (1994) 4831–4837.
- [80] A. Gavezzotti, *Acc. Chem. Res.* 27 (1994) 309–314.
- [81] Z. Mardani, V. Golsanamlou, S. Khodavandegar, K. Moeini, A.M.Z. Slawin, J.D. Woollins, *J. Coord. Chem.* (2018) 1–15.